LTE Radio and Network Planning: Basic Coverage and Interference Constraints

Fernando J. Velez[1] and Daniel Robalo[1]
[1] Instituto das Telecomunicações - DEM
Universidade da Beira Interior
Faculdade de Engenharia
6201-001 Covilhã, Portugal
fjv@ubi.pt, robalodaniel@gmail.com

Jessica Acevedo Flores[1,2]
[2] Universidad Católica San Pablo
Electronics & Telecommunications
Engineering School
Arequipa, Peru
jacevedo@ucsp.edu.pe

***Abstract*—In the cellular planning process, the UL and DL the values from carrier-to-noise-plus-interference ratio (CNIR) from/at the mobile station are very important parameters. From a detailed analysis of its variation with the coverage and reuse distances for different values of the Chanel Quality Indicator (CQI) and given empirical propagation models, an evaluation of the possible range for the reuse pattern is performed for the DL. By considering the CQI and reference CNIR requirements recommended by 3GPP, DL peak bit rates along with the Transport Block Size (TBS) assumed for single stream and bandwidth of 5 MHz, physical and supported throughputs are analysed. These formulations shows the clear decrease of the supported throughput for the longest coverage distances in the LTE 2.6 GHz band, a behaviour that is not so clear at 800 MHz, and gives useful indications to the optimization of the use of different frequency bands in the optimization of carrier aggregation between two different bands in LTE-A scenarios.**

Keywords—LTE; CNIR; radio and network planning; system capacity

I. INTRODUCTION

In nowadays wireless cellular networks, not only mobile services and applications are more and more used by consumers each year, leading to an expansion of mobile data traffic, but the pace at which it is growing is accelerating. According to [1], in 2013 mobile data traffic was nearly 18 times the size of the entire global Internet in 2000. One Exabyte of traffic traversed the global Internet in 2000, and in 2013 mobile networks carried nearly 18 Exabyte's of traffic. In 2013 alone, 526 million mobile devices and connections were added, the global mobile data traffic grew 81 % and mobile video represented 53 % of all mobile traffic and by 2018 it will reach 69 %. Moreover, mobile-connected devices exceed the world's population by 2014. Monthly mobile data traffic will reach 15.9 Exabyte's by 2018 and between 2013 and 2018 the annual growth rate is 61 %, i.e., mobile data traffic will increase nearly 11-fold between 2013 and 2018. These statistics show beyond the shadow of a doubt that wireless and cellular networks technologies need to be enhanced to support such demands. As such, this paper gives contributions to the basic limits of the optimization and planning of 4G cellular networks in a context of heterogeneous Long Term Evolution (LTE) [2] and spectrum management. LTE provides seamless Internet Protocol (IP) connectivity between user equipment (UE) and the packet data network (PDN), and an air interface based on Orthogonal Frequency Division Multiplexing (OFDM) in the downlink (DL) and single-carrier frequency-division multiple access (SC-FDMA) in the uplink (UL), both providing high flexibility in the frequency-domain scheduling. LTE has the flexibility to support time-/frequency-division duplexing (TDD/FDD) and half-duplex FDD schemes.

The main goal of cellular coverage is to offer access to mobile users in a cell, while guaranteeing quality of the received signal in both DL and UL directions, even for the users at the cell edge. As resources, e.g., radio frequency channels, need to be reused in different geographical zones (but not in the closest proximity), the impact of interference among co-channel cells needs to be evaluated in both DL e UL directions. Furthermore, this interference is heavier in users at cell edge, who may suffer from low connection quality.

Therefore, a comprehensive study on the variation of the UL/DL carrier-to-noise-plus-interference ratio (CNIR) from/at the Mobile Station (MS) with different system parameters is critical in the context of LTE planning. In this work, we are just considering DL. The variation of CNIR with the coverage and reuse distances is analysed for different values of the Channel Quality Indicator (CQI). Table I shows the CQI and reference CNIR requirements recommended by 3GPP for DL, as well as the spectral efficiency, S_{ef}.

TABLE I. MINIMUM CNIR, MODULATION AND SPECTRAL EFFICIENCY VERSUS CQI, FOR LTE, AND VALUES FOR THE VERTICAL ASYMPTOTE

CQI	$CNIR_{min[dB]}$	Modulation	S_{ef}	$R_{asymptote[m]}$ $f = 800$ MHz	$R_{asymptote[m]}$ $f = 2.6$ GHz
0		out of range	0		
1	-4.63	QPSK	0.15	9,359	4,432
2	-2.60	QPSK	0.23	8,009	3,793
3	-0.12	QPSK	0.38	6,621	3,135
4	2.26	QPSK	0.60	5,515	2,612
5	4.73	QPSK	0.88	4,563	2,161
6	7.53	QPSK	1.18	3,680	1,743
7	8.67	16-QAM	1.48	3,372	1,597
8	11.32	16-QAM	1.91	2,751	1,303
9	14.24	16-QAM	2.41	2,199	1,041
10	15.21	64-QAM	2.73	2,041	967
11	18.63	64-QAM	3.32	1,570	744
12	21.32	64-QAM	3.90	1,277	605
13	23.47	64-QAM	4.52	1,083	513
14	28.49	64-QAM	5.12	737	349
15	34.60	64-QAM	5.55	461	218

978-1-4673-8451-3/15/$31.00 ©2015 IEEE

Table II presents DL/UL peak bit rates along with Transport Block Size (TBS) considered for single stream and bandwidth of 5 MHz. Power and gains assumed in the considered LTE scenario are presented in Table III for 800 MHz/2.6 GHz LTE.

TABLE II. DL AND UL PEAK BIT RATES WITH TBS CONSIDERED FOR SINGLE STREAM AND A BANDWIDTH OF 5 MHZ-25 RESOURCE BLOCKS

Modulation	DL peak rates [Mbps]	UL peak rates [Mbps]
QPSK	4	4.4
16-QAM	7.7	12.6
64-QAM	18.3	18.3

TABLE III. POWER, GAIN AND NOISE PARAMETERS

Parameters	f = 800 MHz	f = 2.6 GHz
$P_{t[\mathrm{dBW}]}$	13	13
$G_{t[\mathrm{dBi}]}$	3	3.5
$G_{r[\mathrm{dBi}]}$	0	0
$BW_{[\mathrm{MHz}]}$	5	5
$N_{f[\mathrm{dB}]}$	8	8

The remainder of the paper is organized as follows. Section II presents an overview of the considered propagation models. Section III addresses the interference, noise and frequency reuse trade-offs involved in LTE radio and network planning considering different MCSs. Section IV presents a detailed analysis of LTE system capacity considering assumptions for the different levels of CQIs, and discusses results for the equivalent supported throughput as a function of the coverage distance. Finally, conclusions are drawn in Section V.

II. OVERVIEW OF THE PROPAGATION MODELS

The selection of a suitable radio propagation model for LTE is of crucial importance, and many models have been developed to characterize Radio Frequency (RF) environments and allow for the prediction of the RF signal strength. A radio propagation model describes the behaviour of the signal while it is transmitted from the transmitter towards the receiver. It predicts large-scale coverage for radio communications systems in cellular applications and gives a relation between the distance of transmitter and receiver and the path loss. From such a relation, one can get an idea about the allowed path loss and the maximum cell range. Path loss depends on the condition of environment (urban, rural, dense urban, suburban, open, forest, sea, etc.), operating frequency, atmospheric conditions, indoor/outdoor and the distance between the transmitter and receiver, among other factors.

Regarding the development of LTE, for both network planning and predicting achievable performance in typical deployment scenarios, realistic modelling of propagation characteristics is an essential factor to consider. Before implementing, the output from the design and confirming planning of wireless communication systems, accurate propagation characteristics of the environment should be identified. Additionally, to select the appropriate and reliable propagation model would improve the frequency reuse as well.

In the first approach, the radio channel follows the widely used ITU radio propagation COST-231 Hata model for its accurateness and simplicity. In [3], a comparison among different path loss models was carried, demonstrating that COST-231 Hata model offers lower path loss, in dB [4]-[6], with an overall better performance for frequencies up to 3.5 GHz. Therefore, we consider this model in our study for the two selected frequency bands, 800 and 2600 MHz. For medium size cities, the model is given by the following equation:

$$L_{[dB]} = 40\,(1 - 4\cdot 10^{-3}\cdot D_{hb[Km]})\log_{10}(d_{[km]}) - \\ - 18\cdot\log_{10}(D_{hb[km]}) + 21\cdot\log_{10}(f_{[MHz]}) + 80 \quad (1)$$

for urban and suburban scenarios, outside the high rise core, where the buildings are of nearly uniform height. In (1), d is the base station (BS)/user equipment (UE) separation in km, f is the carrier frequency, and D_{hb} is the BS antenna height, measured from the average rooftop level.

Considering two carrier frequencies, 800 MHz and 2.6 GHz, D_{hb} = 15 m and a UE antenna of 1.5 m, one obtains the following path loss model:

$$L_{800\ \mathrm{MHz}\,[\mathrm{dB}]} = 119.16 + 37.6\cdot\log_{10}\left(d_{[km]}\right) \\ L_{2\ \mathrm{GHz}\,[\mathrm{dB}]} = 128.1 + 37.6\cdot\log_{10}\left(d_{[km]}\right) \quad (2)$$

Besides, the modified Friis model is considered together with the COST-231 Hata model. For dimensioning purposes, the attenuation, is computed as follows:

$$L = 32.4 + 30\cdot\gamma + 20\cdot\log_{10}(d_{[km]}) + \gamma_{rain}\cdot d + \\ + \gamma_{fog}\cdot d + \gamma_{snow}\cdot d + 20\cdot\log_{10}(f_{GHz]}) \quad (3)$$

where γ it is the propagation exponent, γ_{rain} and γ_{fog} are the specific attenuations due to rain and fog, γ_{snow} is the specific attenuation due to snow (all these specific attenuations are expressed in dB/km), and f is the frequency in GHz [7].

The values for the parameters are as follows: γ=3 [8], [9]. They are obtained empirically and account for site-specific factors, γ_{rain} = 0.0811 dB/km [10], γ_{fog} = 0.01 dB/km. As $\gamma_{fog} << \gamma_{rain}$, it can be neglected [7]; γ_{snow} is neglected for frequencies below 30 GHz [3]. d varies between 0 and 6 km. Then we obtain:

$$L_{800\ MHz\,[dB]} = 120.46 + 20\cdot\log_{10}(d_{[km]}) + \gamma_{rain}\cdot d_{[km]} \\ L_{2.6\ GHz\,[dB]} = 130.69 + 20\cdot\log_{10}(d_{[km]}) + \gamma_{rain}\cdot d_{[km]} \quad (4)$$

III. CELLULAR PLANNING

An efficient use of the radio frequency spectrum requires choosing a frequency reuse scheme that leads to coverage guarantee, and improved system capacity whilst minimizing the interference. Conventionally, most authors uncouple the analysis of the carrier-to-noise ratio (coverage problem) aspects from the analysis of the carrier-to-interference ones (frequency reuse). Thus, interference is not considered in coverage while noise is not considered when addressing the frequency reuse.

On the one hand, not considering the interference in the coverage problem means that the maximum coverage distance is obtained without allowing for extra margin for the interference, which is a critical limitation for the dimensioning process of a cellular system. On the other hand, the absence of noise in the interference analysis is unrealistic, as noise is always present in communications. As there would be limitations arising from an independent analysis, cellular planning has to simultaneously consider carrier-to-noise and carrier-to-interference constraints. Improvement techniques as sub-channelization and sectored antennas, can be considered to improve coverage and avoid interference.

A. Formulation for Carrier-to-noise-plus-interference Ratio

This section addresses aspects related to the analysis of the cell coverage distance (or cell radius), R, the co-channel reuse factor, r_{cc}, the ratio between the reuse and the coverage distances, the reuse pattern, K, for several levels of LTE MCS. The conclusions taken out would facilitate the appropriate selection of the reuse pattern and an efficient frequency planning. The carrier, interference and noise powers (C, N and I, respectively) are considered.

If one considers the interference-to-noise ratio, defined by:

$$M = \frac{I}{N} \tag{5}$$

and the equation for the carrier-to-noise-plus-interference ratio (CNIR) to be used in the dimensioning process is the following:

$$\left(\frac{C}{N+I}\right) = \left(\frac{C}{N}\right)_{min} \tag{6}$$

Equation (6) can be re-written in the two following ways

$$\left(\frac{C}{N}\right) = \left(\frac{C}{N}\right)_{min} (1 + M) \tag{7}$$

$$\left(\frac{C}{I}\right) = \left(\frac{C}{N}\right)_{min} (1 + M^{-1}) \tag{8}$$

In (6) one is considering the model for CNIR from [11] while assuming that weights for noise and interference are the same.

From equation (7) one obtain the following equation for the interference-to-noise ratio:

$$M(R) = \left(\frac{\left(\frac{C(R)}{N}\right)}{\left(\frac{C}{N}\right)_{min}}\right) - 1 \tag{9}$$

where $C(R)=P_R(R)$ is computed by applying the modified Friis model with $\gamma = 3$, the hypothesis followed in this Section for suburban environments. Values of $M(R)$ are proportional to the interference still tolerable for a given coverage distance R while (still) agreeing with the quality requirements for a given MCS.

With a hexagonal cell topology, in the DL, Figure 1, as the distance associated with interference is D, i.e., the reuse distance itself, the carrier-to-interference ratio can be given by:

$$\frac{C}{I} = \frac{1}{2(r_{cc}+1)^{-\gamma}+2r_{cc}{}^{-\gamma}+2(r_{cc}-1)^{-\gamma}} \approx \frac{r_{cc}{}^{\gamma}}{6} \tag{10}$$

where r_{cc} is the co-channel reuse factor, given by:

$$r_{cc} = \frac{D}{R} \tag{11}$$

The approximate expression in (10) is very useful in practice. It is worthwhile to note that, for hexagonal reuse geometries, the reuse pattern is given by

$$K = r_{cc}{}^{2}/3 \tag{12}$$

As a horizontal asymptote arises in the analysis of the curves of r_{cc} as a function of the coverage distance, R, it is important to present the mathematical details associated to it. To compute the horizontal asymptote in the chart from $r_{cc}(R)$, one has to consider that $R \to 0$. From (9), if $R \to 0$ then $M \to +\infty$, and $M^{-1} \to 0$.

On the one hand, for the DL, in the limit, one obtains:

$$\lim_{R\to 0} r_{cc} = \sqrt[\gamma]{6 \cdot \left(C/N\right)_{\min}} \tag{13}$$

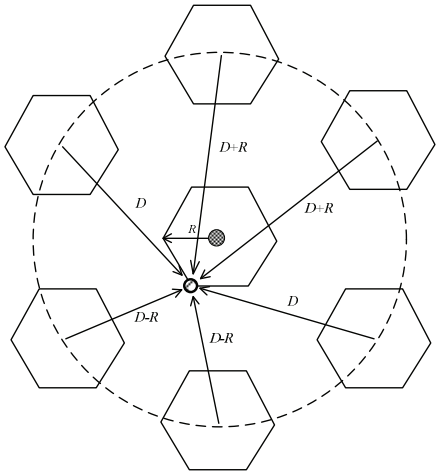

Fig. 1. Co-channel interference in the worst-case for the DL.

By considering (12), it is straightforward to conclude that, for each value for the propagation exponent, the reuse pattern, K, only depends on the MCS through the value of the corresponding minimum carrier-to-noise ratio, as well as on the cellular interference geometry.

While the asymptotic reuse factor is associated with the upper bound for system capacity, the maximum coverage distance is associated with the carrier-to-interference-plus-noise ratio at the cell boundary when the interference is null. Since the interference-to-noise ratio, M, represents the interference that can still be tolerated for a given R, in the limit, the maximum coverage distance for which no extra interference is tolerated is obtained when $I(R) \to 0$, i.e., when $M(R) \to 0$ (meaning that $M_{[dB]} \to -\infty$). Hence, the vertical asymptotes for the $M(R)$ and $r_{cc}(R)$ charts is the following:

$$R_{asymptote} = R_{M\to 0} \tag{14}$$

It is obtained by solving the following equation:

$$M(R) = \frac{\left(C(R)/N\right)}{\left(C/N\right)_{\min}} - 1 = 0 \tag{15}$$

or, in a simplified way:

$$C(R)/N = \left(C/N\right)_{\min} \tag{16}$$

By comparing this equation (valid only when $M \to 0$) with equation (7), one concludes that only considering the carrier-to-noise ratio to determine the coverage distance, R, is inadequate in systems where interference is relevant, as equation (16) corresponds to a null interference-to-noise ratio, M. If a cellular system was dimensioned this way there would not be an extra margin for interference, represented by $M = I/N$. Finally, it is a worth noting that, for a given propagation exponent, the maximum coverage distance corresponding to the vertical asymptote, $R_{asymptote}$, depends not only on the MCS but also on the noise power, N. This is the reason why the reduction of the noise power through sub-channelization, i.e., through reduction of the RF bandwidth, can be so important.

B. Interference-to-noise Ratio and Reuse Pattern

By using (9), one obtains the curves for the DL interference-to-noise ratio, considering the Friis and Hata models for the 800 MHz and 2.6 GHz frequency bands. The

considered propagation exponent for the modified Friis model is γ =3.

Considering the values in Table II, and considering both models we obtained the values of interference-to-noise-ratio, M, in the DL for f = 800 MHz which depends on the CQI value and the MCS associated to it. Table II also presents the corresponding values for the vertical asymptote, $R_{asymptote}$. It is observed a relevant decrease of the values for the vertical asymptote (maximum R) as the MCS level increases, which is compatible with the lowest values for $CNIR_{min}$.

By applying (11) and (12) to the DL one obtains the charts for $r_{cc}(R)$ and $K(R)$ from the Figures in the results. Charts for the interference-to-noise ratio, $M(R)$,are also presented by considering (9). On the one hand, these results are obtained for the 800 MHz frequency band, and considering the modified Friis (γ=3) and Hata models, as shown in Figures 2-5. On the other hand, Figures 6-9 analyse the 2.6 GHz frequency band whilst considering the same empirical propagation models.

It is clear that, at 800 MHz, for the shortest coverage distances, the interference-to-noise ratio is lower for modified Friis propagation model, but it becomes highest than for the Hata model for the largest coverage distances.

As a consequence, for the modified Friis and Hata models, with CQI up to 7, low reuse patterns are achievable while, with CQI 8, K lower than 7 is obtained for Rs up to circa 1500 and 1400 m, respectively.

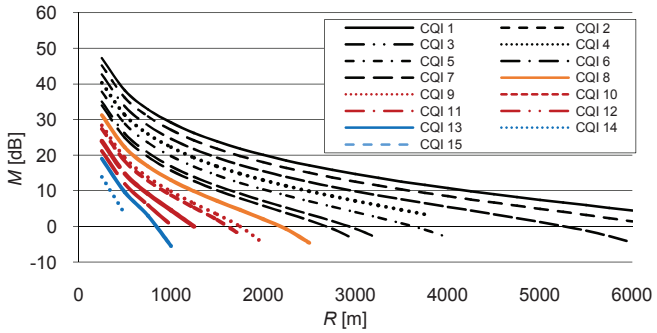

Fig. 2 Interference to noise ratioas a function of the coverage distance with CQI as a parameter for DL, in the 800 MHz band and Friis model.

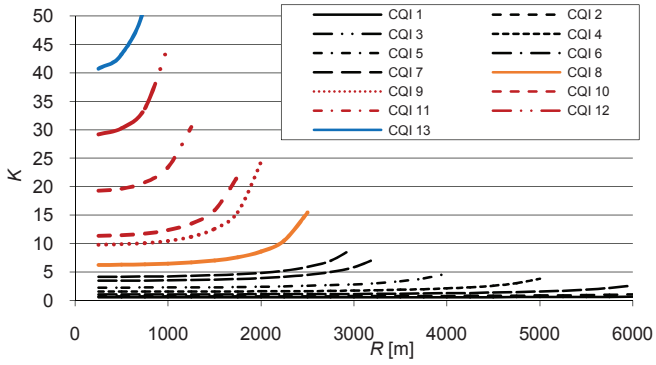

Fig. 3 Reuse pattern as a function of the coverage distance with CQI as a parameter for DL, in the 800 MHz frequency band and Friis model

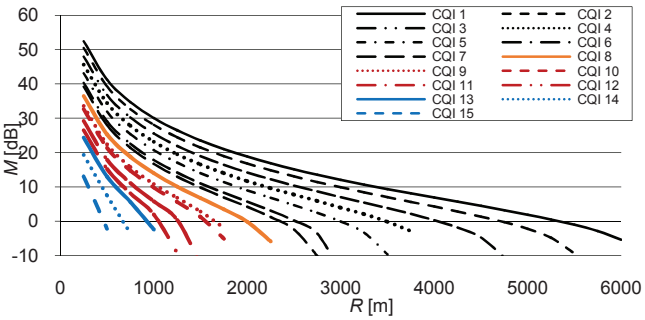

Fig. 4 Interference to noise ratioas a function of the coverage distance with CQI as a parameter for DL, in the 800 MHz band and Hata model.

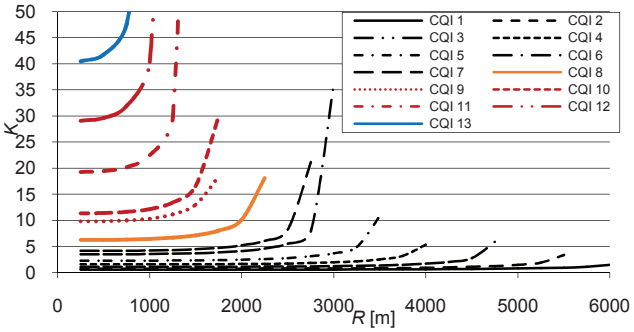

Fig. 5 Reuse pattern as a function of the coverage distance with CQI as a parameter for DL, in the 800 MHz frequency band and Hata model.

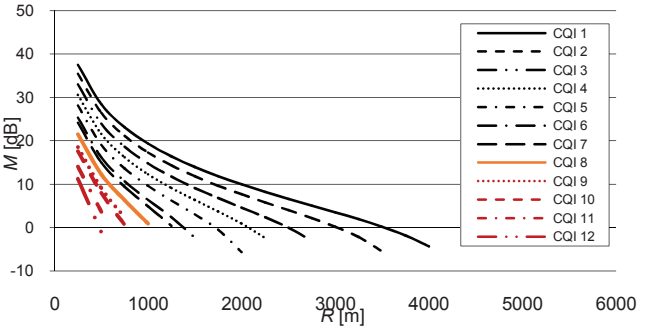

Fig. 6 Interference to noise ratio as a function of the coverage distance with CQI as a parameter for DL, in the 2.6 GHz band and Friis model.

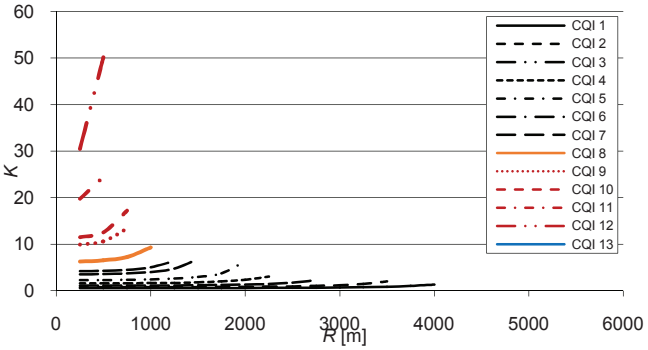

Fig. 7 Reuse pattern as a function of the coverage distance with CQI as a parameter for DL, in the 2.6 GHz frequency band and Friis model.

At 2.6 GHz, M is lower than at 800 MHz but behaviour for the shortest and longest coverage distances is similar to the former one at 800 MHz.

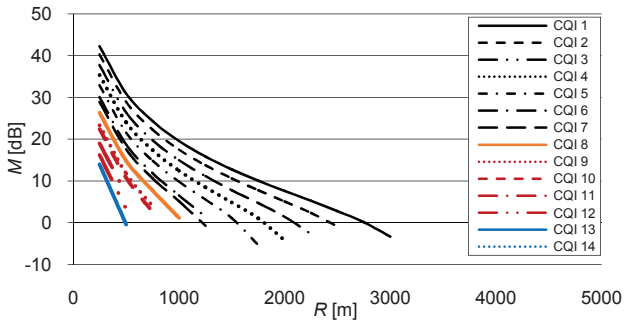

Fig. 8 Interference to noise ratio as a function of the coverage distance with CQI as a parameter for DL, in the 2.6 GHz band and Hata model.

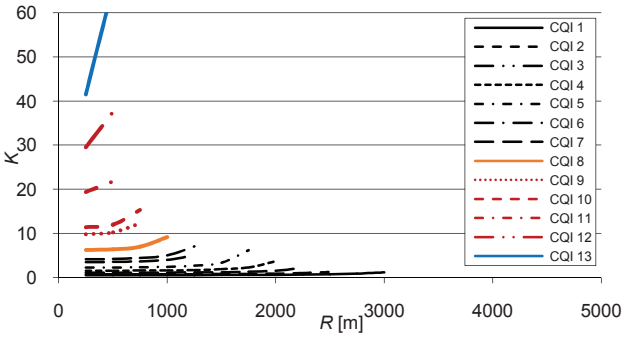

Fig. 9 Reuse pattern as a function of the coverage distance with CQI as a parameter for DL, in the 2.6 GHz frequency band and Hata model.

C. *Supported Throughput and its Dependence on CNIR*

From the analysis of the results from Figs. 10 and 11, it is clear that achievable values for *CNIR* are more favourable for the 800 MHz frequency band.

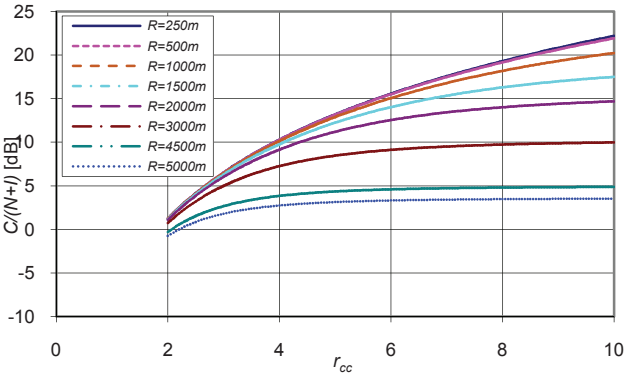

Fig. 10 CNIR for the DL in the 800 MHz frequency band.

Hence, in the step transitions observed in the curves for throughput (different CQI $CNIR_{min}$), the achieved physical throughput increases first (for lower coverage distance, R) than at 2.6 GHz, as shown in Fig. 12 (example for 800 MHz).

IV. Detailed Analysis of System Capacity

While previous Sections analyse the individual influence of each MCS, it is also worthwhile to study the overall impact of different MCS. Following the formulation from [4] for an implicit function procedure to compute supported throughput, the LTE system capacity is analyzed at both 800 MHz and 2.6 GHz considering the COST-231 propagation model.

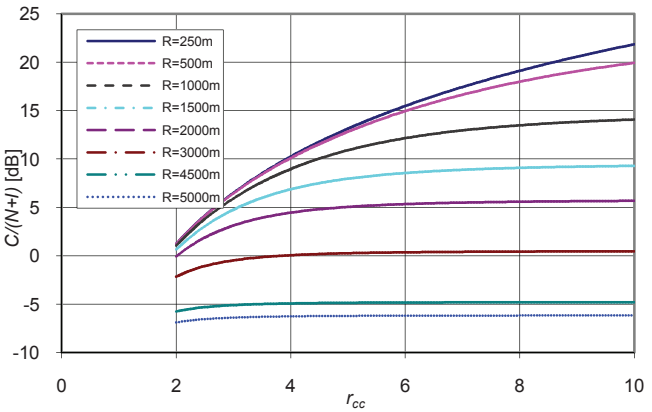

Fig. 11 CNIR for the DL in the 2.6 GHz frequency band

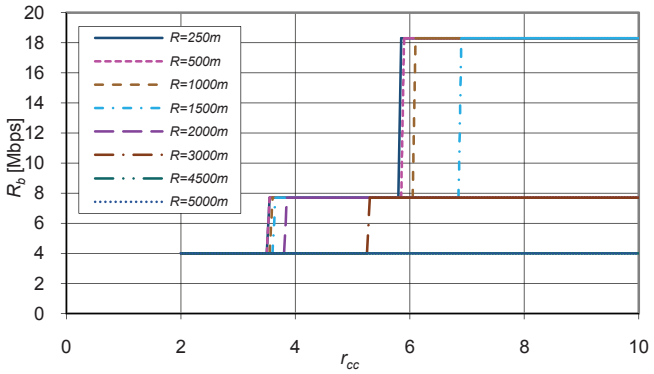

Fig. 12 Physical throughput for the DL in the 800 MHz in band.

The analysis only considers the supported throughput for K equal to 1, 3 and 7. One considers the values for P_t, G_r, BW and N_f from Table III but the transmitter antenna gain is now G_t=14 dBi. The COST-231 Hata model is assumed. Additionally, to map the reference CNIR into supported throughput one has considered a formulation slightly more elaborated than in Section III and assumed the values provided by [5], more specifically Tables 7.1.7.1-1 and 7.1.7.2.1-1.

By extrapolating the gathered information it is possible to map the CNIR into CQI, MCS index, Modulation Order Transport Block Size (ITBS) index and TBS. Furthermore, assuming TTI = 1 ms the throughput (goodput) is obtained by multiplying the TBS by this value, and as a 5 MHz bandwidth is considered, i.e., 25 PRBs, column NPRB = 25 from Table 7.1.7.2.1-1 from [5] is also assumed.

The number of coverage rings is equal to 27, i.e., equal to the number of ITBS, as each index corresponds to a different value of the throughput. Figure 13 shows the values obtained for the 800 MHz carrier component (CC), whereas Figure 14 shows the results for the 2.6 GHz CC. Overall, the main difference between both CCs is the decline of the supported throughput as a function of the distance. This decay is apparent it both cases, however, it is more noticeable at 2.6 GHz. This difference is expected since the path loss at 2.6 GHz is higher than the one at 800 MHz.

Furthermore, although K = 7 presents the highest values of the supported goodput, it is also the reuse pattern which presents the most evident reduction as a function of the distance. On the opposite side of the previous remarks, the case

K = 1 shows slightly no reduction of the supported throughput with the distance, but presents the lowest values of the three addressed reuse patterns. Finally, K = 3 presents a mixture of the behaviour form previous cases.

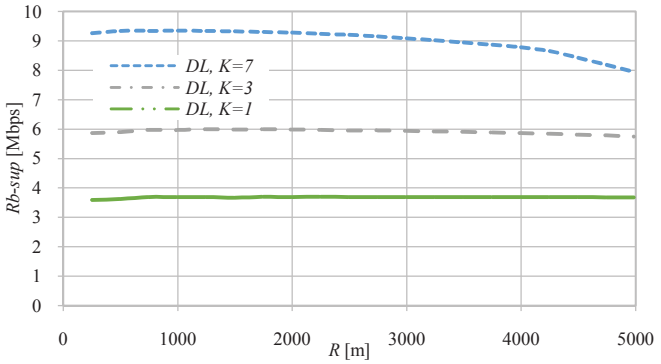

Fig. 13 Comparison of the equivalent supported throughput between cells for K = 1, 3 and 7 at 800 MHz.

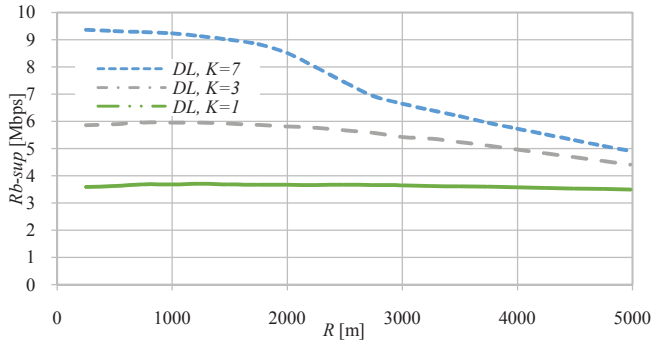

Fig. 14 Comparison of the equivalent supported throughput between cells for K = 1, 3 and 7 at 2.6 GHz.

On the one hand, the obtained values are slightly affected by the distance at 800 MHz, whereas at 2.6 GHz the reduction is more apparent. On the other, the supported values for the goodput are in-between the ones obtained with K = 1; 7. It is also interesting to note that the maximum supported throughput obtained at the lowest addressed distance, R = 250 m, is approximately the same for both CCs, i.e., 3.6, 5.9 and 9.3 Mbps in the DL, for K = 1, 3 and 7, respectively. In perspective, considering R = 2500 m and K = 7 the achieved results are 9.2 Mbps (800 MHz CCS) and 7.4 Mbps (2.6 GHz CCs) in the DL.

V. Conclusion

This work has presented a comprehensive study on the variation of the carrier-to-noise-plus-interference ratio (CNIR) with different LTE system parameters. For cellular radio and network planning purposes, the UL and DL CNIRs from/at the mobile station are very important parameters. From a detailed analysis of its variation with the coverage and reuse distances for different modulation and coding schemes in the DL and given empirical propagation models, an evaluation of the possible range for the reuse pattern has been performed. By considering the CQI and reference CNIR requirements recommended by 3GPP. DL peak bit rates along with the Transport Block Size assumed for single stream and bandwidth of 5 MHz, an analysis of the physical and supported throughputs has been performed. The lowest CNIR for longer distances at 2.6 GHz implies that, in the step transitions observed in the curves for throughput (different $CNIR_{min}$ thresholds), at 800 MHz the achieved physical throughput increases first (for the lowest Rs) than at 2.6 GHz. One can learn that the main difference between the two bands is the clear decrease of the supported throughput for the longest coverage distances in the 2.6 GHz band, a behaviour that is not so clear at 800 MHz.

These formulations show the basic limits for system capacity from LTE systems and gives hints to the optimization of the use of different frequency bands in the optimization of carrier aggregation in LTE-A scenarios, as the ones established in [11], [12].

Acknowledgment

This work has been partially supported and funded by ECOOP, UID/EEA/50008/2013, NEUF, OPPORTUNISTIC-CR, PROENERGY-WSN, CREaTION, COST IC 1004, EFATraS, HANDCAD and ORCIP.

References

[1] Cisco Visual Networking Index: Global Mobile Data Traffic Forecast Update, 2013-2018, white paper, Feb. 2014.

[2] The 3rd. Generation Partnership Project (3GPP). [Online]. Available: www.3gpp.org.

[3] Ramjee Prasad, Fernando J. Velez, *WiMAX Networks: Techno-economic Vision and Challenges*, Springer, Dordrecht, The Netherlands, 2010 (ISBN: 978-90-481-8751-5).

[4] Fernando J. Velez, A. Hamid Aghvami and Oliver Holland, "Basic Limits for Fixed Worldwide Interoperability for Microwave Access Optimization Based in Economic Aspects," IET Communications – Special Issue on WiMAX Integrated Communications, vol. 4, no. 9, June 2010, pp. 1116-1129 (available online DOI 10.1049/iet-com.2009.0190).

[5] 3GPP TS 36.213 v12.2.0, Physical Layer Procedures (Release 12). The 3rd. Generation Partnership Project. Technical Specification Group Radio Access Network, Jun. 2014.

[6] COST Action 231. "Digital mobile radio. Towards future generation systems—Final report"

[7] Fernando J. Velez, Vitor Carvalho, Dany Santos, Rui P. Marcos, Rui Costa, Pedro Sebastião and António Rodrigues, "Planning of an IEEE 802.16e Network for Emergency and Safety Services," in *Proc. of 3G 2005 - 6th IEE International Conference on 3G Mobile Communication Technologies*, London, UK, Oct. 2005.

[8] Safdar Nawaz Khan Marwat, LTE Channel Modelling for System Level Simulations, Master thesis, University of Bremen, Sept. 2011.

[9] Guillaume de la Roche, Andres Alayón-Glazunov, Ben Allen, *LTE-Advanced and Next Generation Wireless Networks*, John Wiley and Sons, 2013.

[10] Carlos Salema, *Microwave Radio Links*, John Wiley & Sons, Hoboken, New Jersey, USA, 2003.

[11] Jessica Acevedo, Daniel Robalo, Fernando J. Velez, "Transmitted Power Formulation for the Optimization of Spectrum Aggregation in LTE-A over 800 MHz and 2 GHz Frequency Bands," *Wireless Personal Communications*, June 2015.

[12] Daniel Robalo and Fernando J. Velez, "Economic trade-off in the optimization of carrier aggregation with enhanced multi-band scheduling in LTE-Advanced scenarios," *EURASIP Journal on Wireless Communications and Networking*, vol. 189, no. 1, 2015.